Chapter 13
Optical Manipulation

Paul Bartlett

13.1 Introduction

Manipulating, analysing and organising the mesoscopic structure of materials is probably the most challenging problem currently facing soft matter science. Soft materials, which include polymers, colloids, microemulsions, micellar systems and their aggregates, are characterised by a wide range of length scales, ranging from tens of nanometres to tens of microns, forces from femtonewtons to nanonewtons and timescales which span microseconds to hours. Organising material on these scales has traditionally only been possible through a subtle *chemical* control of interactions and dynamics. However in the last two decades a new generation of optical techniques has emerged that allow soft matter scientists to *physically* reach down into the microscopic world, grab, move and transform dielectric objects at will, with almost nanometre precision. This chapter summarises the ideas behind these new powerful optical manipulation techniques and highlights a few recent applications in soft matter science. More detailed reviews of this area are included in the articles by Grier [1] and Molloy and Padgett [2] while recent developments in optical manipulation techniques have been summarised by Dholakia *et al.* [3].

13.2 Manipulating Matter with Light

Moving objects with light seems, at first sight, the stuff of science fiction stories. Indeed 'tractor beams' play a major role in classic Sci-Fi tales such as Star Trek where the *U.S.S. Enterprise's* laser beam is used to pull in crafts, tow another ship or hinder the escape of an enemy spacecraft [4]. The stories may be a little fantastical but the science is sound. Light can move matter because photons carry a momentum. Each photon of wavelength λ has a momentum $p = h/\lambda$ where h is Planck's constant. Illuminating an object leads to a change in the direction of light as a result of refraction, reflection and diffraction. The incident momentum of the beam of photons is changed and so from Newton's laws of motion the object must also experience a force. Of course, the forces are not large enough to move spaceships (unless the beam is phenomenally intense) but for small objects, such as micron-sized particles, the forces are sufficient to allow them to be moved at will.

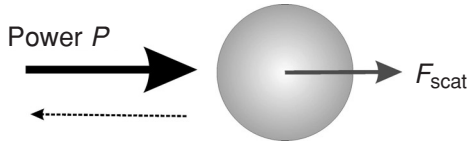

Figure 13.1 Optical scattering force on a sphere.

A very simple calculation, illustrated in Figure 13.1, confirms the magnitude of optical forces. Imagine a light beam of power P incident on a microscopic sphere. As every photon carries an energy $h\nu$ the number of photons incident on the particle per second is $P/h\nu$. If a fraction q of the beam is reflected back then the momentum transferred to the particle leads to a scattering force on the particle of magnitude

$$F_{\text{scat}} = 2\left(\frac{P}{h\nu}\right) \times \left(\frac{h}{\lambda}\right) \times q = \frac{2qnP}{c} \tag{13.1}$$

where c is the velocity of light and n is the refractive index of the medium. Inserting typical values gives a crude estimate of the strength of optical forces. Assuming, for instance, a 100 mW laser beam focused on a dielectric sphere of radius λ, for which q is of order 0.05 [5], yields an optical force of about 40 pN. Although this force is obviously far too small to move anything as large as a spacecraft, at the microscopic level such piconewton-level forces can have a very significant effect. To see this we need to consider the typical magnitudes of forces found in colloidal systems.

Figure 13.2 shows schematically the range of typical forces encountered in soft matter science. Rupture of covalent bonds requires forces of order 1–2 nN while forces of about 20–50 pN are sufficient to unravel polymer chains, convert DNA from a double helix to a ladder or to break most van der Waals interactions. Colloidal forces are typically an order of magnitude smaller with the interaction forces between micron-sized colloidal particles being on a scale of a few ten to hundreds of femtonewtons. Probably the weakest forces encountered are those originating from gravity, where the sedimentation force on a colloidal particle is

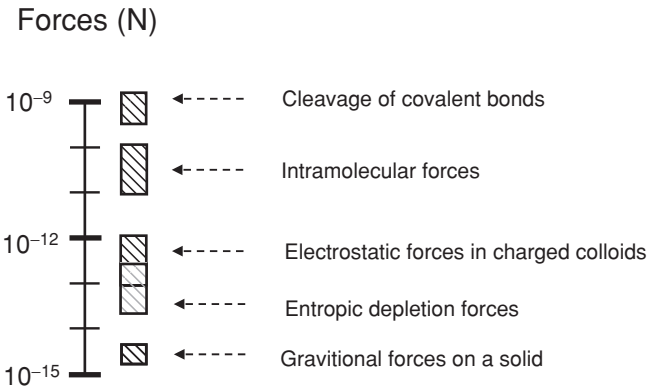

Figure 13.2 The strengths of forces encountered in soft matter science.

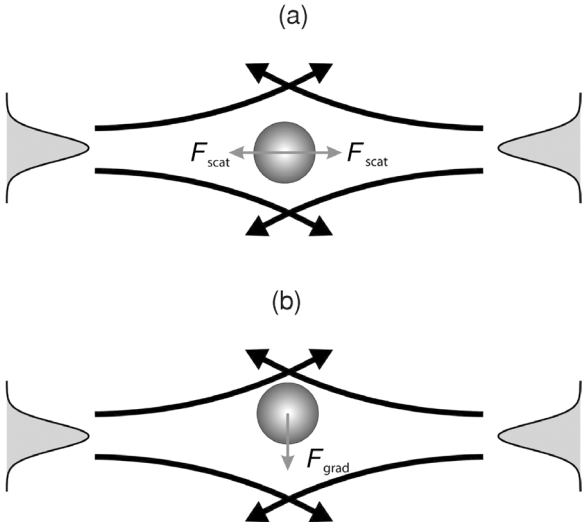

Figure 13.3 An optical trap generated by two counter-propagating beams. (a) At the equilibrium position the axial scattering forces F_{scat} generated by each beam exactly balance, while (b) when the trapped particle is displaced radially there is an unbalanced lateral gradient force F_{grad}.

typically a few femtonewtons. Optical techniques, as we shall see below, may be used to apply and measure forces ranging between ∼10 fN and ∼100 pN making them ideally suited to the study and manipulation of soft matter.

The first three-dimensional optical traps were built by Arthur Ashkin working at Bell Labs in the early 1970s [6]. The trap consisted of two counter-propagating weakly diverging laser beams as shown schematically in Figure 13.3. At the equilibrium point the axial forces F_{scat}, generated by the *scattering* of photons from both beams, exactly balance and the particle is stably trapped. Any motion along the axis leads to a net scattering force which moves the particle towards the equilibrium point (Figure 13.3a). Although this might be expected from our discussion above, Ashkin saw, rather surprisingly, that the particle was also confined radially (Figure 13.3b). This observation, although apparently mundane, is key to the successful development of optical trapping techniques. It was the first demonstration that radiation pressure could also produce a *transverse* force component, which acts perpendicular to the line of the beam. The transverse or *gradient* force, F_{grad}, acts to move the particle to wherever the laser field is the highest. So in the case of the counter-propagating trap any radial displacement of the particle is opposed by gradient forces generated by both beams. The particle is stable against random displacements in all three dimensions and 'optical trapping' had arrived in the laboratory.

While the counter-propagating trap worked, alignment was rather tedious and the need to get optical access from two sides restricted its use. It was therefore a significant breakthrough when Ashkin showed in 1986 [7] that the gradient forces produced near the focus of a *single* tightly focused laser beam could trap a transparent particle in three dimensions. In the last two decades, this technique, now referred to almost universally as 'optical tweezers', has become a mainstream tool in nanotechnology and biology.

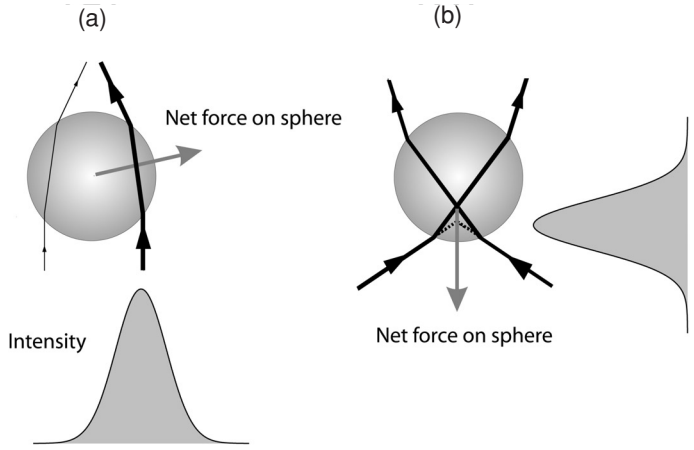

Figure 13.4 Force generation in a single-beam optical gradient trap.

13.3 Force Generation in Optical Tweezers

To understand how a single tightly focused laser trap works, study Figure 13.4. This figure shows the passage of light rays as they travel through a transparent sphere with a high index of refraction. At the surface of the sphere light is refracted and is bent towards the normal on entry and away from the normal on exit, according to Snell's law. Each time the light ray is refracted there is a change in photon momentum and so from Newton's third law the particle will experience an equal and opposite force. Figure 13.4a illustrates the case when the particle is displaced to the left of the centre of the beam. More light is refracted to the left than to the right so the particle experiences a net force directed to the right and towards the centre of the beam. When the particle is moved up, away from the beam focus, as shown in Figure 13.4b, then light rays are refracted upwards which generates a reaction force on the sphere which pulls it towards the beam focus. The net effect is that the motion of the particle is constrained in all three dimensions.

This ray optics approach gives remarkably accurate estimates for the strength of optical trapping provided the sphere is significantly larger than the wavelength of the laser [8]. For smaller particles it is better to use arguments based on the strength of the electric field at the trapped particle [9]. Focusing a laser beam generates an intense electric field at the beam focus, as shown schematically in Figure 13.5. The effect of the electric field is to polarise the trapped sphere and generate a time-dependent induced dipole $\mu = \alpha E$, whose size depends upon the polarisability α of the sphere. To first order, the polarisability α of a sphere of radius r varies like $\alpha \approx (n_p - n_m)r^3$, where n_p and n_m are the index of refraction of the particle and medium respectively. So a sphere with an index of refraction above that of the medium has a positive polarisability.

The effect of the oscillating induced dipole is twofold. First it emits radiation which gives rise to a scattering force on the particle. The intensity of light scattered is proportional to the square of the induced dipole, so the strength of the scattering force scales as the square

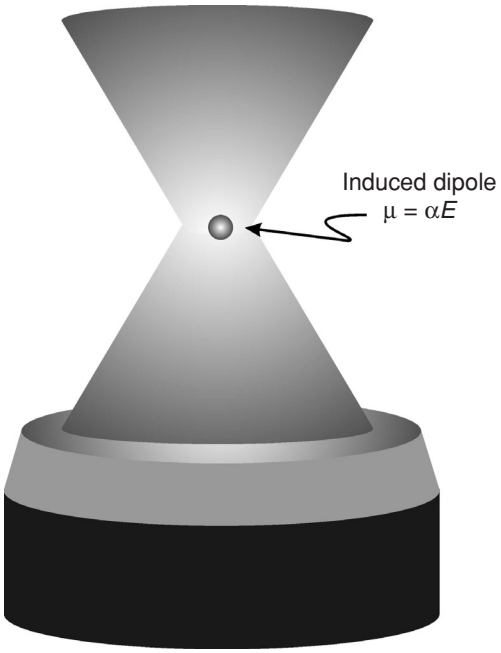

Figure 13.5 A sphere trapped by the intense electric field at the focus of a single-beam gradient trap.

of the polarisability, $F_{\text{scat}} \approx \alpha^2 E^2 \approx (n_p - n_m)^2 r^6 I$ where I is the laser intensity. Although not apparent from this equation, F_{scat} is parallel to the direction of light propagation so the particle is guided along the beam by the scattering force. The second effect arises from the field gradient present near the beam focus. An aligned dipole, which consists of a separated positive and negative centre of charge, experiences no net force when placed in a uniform electric field. However in a spatially varying field the electric fields at the positive and negative centres of charge differ so that there is a net force on the dipole. The strength of this gradient force is $F_{\text{grad}} \approx \mu \nabla E$ which using our earlier expression for the induced dipole is easily seen as equivalent to $F_{\text{grad}} \approx (\alpha/2) \nabla E^2$ (∇ is a differential operator). The gradient force is linear in the polarisability and is directed towards the region of highest light intensity in the case where $\alpha > 0$. For stable three-dimensional trapping we must concentrate on increasing the gradient forces so that they exceed the scattering forces. This cannot be done by simply adjusting the laser intensity since both the scattering and gradient forces vary linearly with intensity. Instead we need to maximise the intensity gradient near the beam focus. This is most readily achieved by using a high numerical aperture microscope objective which brings light from a wide cone angle to a sharp focus. Finally we emphasise that the refractive index of the trapped particle must be higher than that of the surrounding medium to ensure that the gradient force is directed towards the maximum intensity region. An air bubble or generally a particle with a low refractive index is expelled from the beam focus as the gradient forces are reversed.

13.4 Nanofabrication

Optical tweezers offer a highly controlled way of manipulating soft matter systems. There is no direct physical contact with the system, so there is no possibility of contamination. Furthermore, the ability to remotely position colloids in space means that it is now possible to construct new classes of materials. One of the most exciting developments in optical tweezer technology has been the creation of three-dimensional arrays of optical tweezers. These multiple trap systems are created by using a computer-controlled liquid crystal spatial light modulator to generate a highly controlled phase modulator. When illuminated with a single coherent laser beam the outgoing reflected beam is precisely modulated in phase so that when focused in the tweezer plane there is constructive interference between different parts of the beam and an array of tweezers if generated. Using this technique (known as holographic optical tweezers or HOT) more than nearly 2000 traps have been generated in a plane [10].

Holographic optical tweezers are computer controlled and can be reconfigured rapidly so that the array of traps can be adjusted in space and the structure rotated or modified in real time. Figure 13.6 shows, for instance, a sequence of video images of eight spheres trapped at positions corresponding to the corners of a 'tumbling' cube where the resolution of the spatial light modulator allows the unit cell size to be set arbitrarily between 4 and 20 μm.

Such controllable three-dimensional patterning is currently under active investigation as a means of organising nanoparticles into photonic band-gap materials.

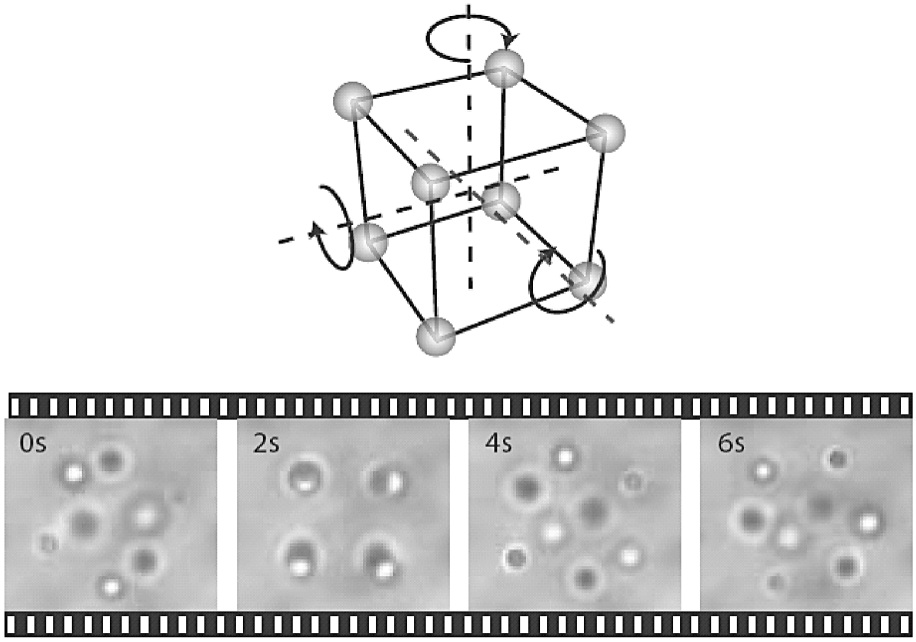

Figure 13.6 Eight silica spheres (diameter 2 μm) trapped at the corners of tumbling simple cubic lattice [11] (reproduced with permission).

13.5 Single Particle Dynamics

For the last few decades much of what we know about the dynamics of soft matter has been derived from bulk techniques such as light, x-ray and neutron scattering which measure the properties of a statistically very large ensemble of particles (typically $> 10^{12}$). The averaging inherent in these measurements means that one cannot measure the entire distribution of particle properties. Single particle techniques offer a wealth of new data on individual properties which allow much more stringent testing of ideas and also offer the potential to reveal entirely new behaviour that is not discernible in averaged results particularly from heterogeneous populations. In this section we show how optical tweezer techniques allow us to measure the dynamics of individual colloidal particles with nanometre spatial and microsecond temporal resolution. We illustrate the power of this method by exploring the heterogeneous dynamics of colloidal gels.

13.5.1 Measuring nanometre displacements

The three-dimensional position of a sphere held in an optical trap can be measured with a resolution of a few nanometres using the four-quadrant photosensor depicted in Figure 13.7.

The sensor relies on interference between the light scattered forward by the particle and the transmitted trapping laser [12]. Motion of the particle within the trap changes the direction of the scattered light and so alters the interference pattern. The interference image is projected onto a four-sector quadrant photodetector. The resulting photocurrents are amplified, and combined to yield voltage signals which are proportional to the X, Y and Z coordinates of the trapped sphere. Because of the intense illumination the resolution is very high and using low noise electronics it is possible to achieve nanometre resolution over

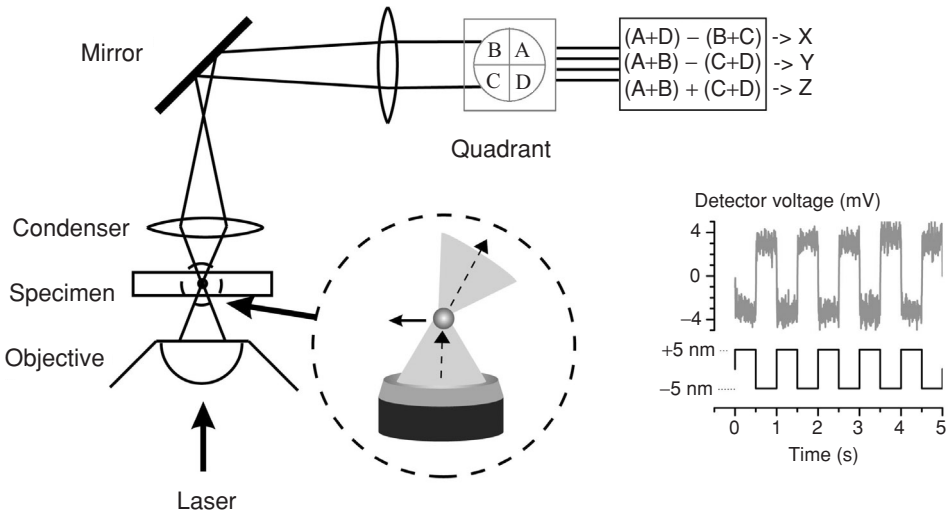

Figure 13.7 Quadrant photosensor detection of particle displacement.

a bandwidth from about 1 Hz to 10 kHz. Figure 13.7 shows the detector response when a sphere is scanned back and forth in 10 nm steps. Clearly the noise level is at the nanometre level.

13.5.2 Brownian fluctuations in an optical trap

A particle held within an optical trap is in fact not fixed but fluctuates in position as a result of a balance between thermal Brownian forces and the optical gradient and scattering forces. The quadrant photosensor provides a very accurate picture of these thermal fluctuations. Figure 13.8 shows an example of the chaotic random trajectory measured for a particle held within an optical trap which can fluctuate about 50 nm around the optical axis.

Analysis of the time-dependent fluctuations of the trapped particle provides a quick and accurate method to characterise the strength of the optical trap. The gradient force provides a restoring force which, over distances of several hundred nanometres, is a linear function of the displacement x of the particle from the centre of the beam focus so that $F_{\text{grad}} = -kx$ where k is the stiffness or force constant of the optical trap. The trapped particle is essentially bound by a weak spring to the centre of the trap. The particle however does not oscillate (as it would in air or a vacuum) because the motion is heavily damped by the surrounding viscous liquid medium. Figure 13.9a shows that the particle fluctuates

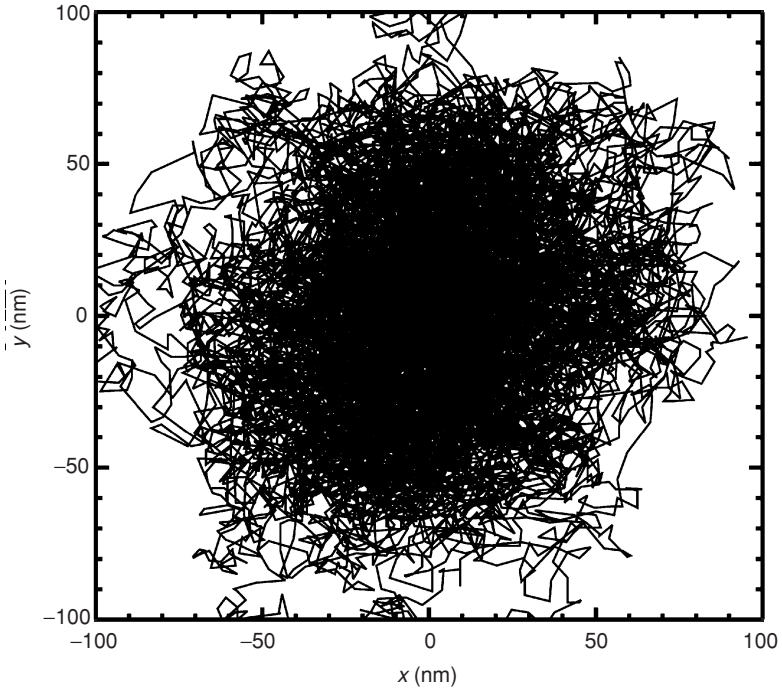

Figure 13.8 The Brownian trajectory (measured for 0.8 s) of a PMMA microsphere of diameter 0.8 μm held in an optical trap.

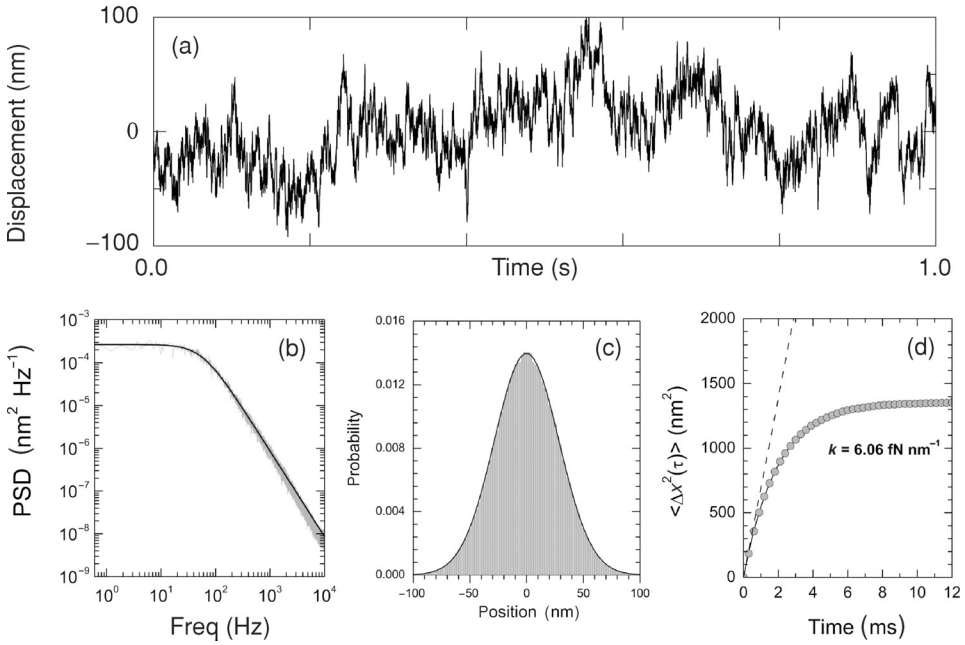

Figure 13.9 The thermal fluctuations of a particle held within an optical trap.

on a timescale of order 10 ms but the motion is very erratic as a consequence of random solvent collisions. The statistics of the thermal fluctuations however reveal the nature of the interaction between the particle and the optical trap. Spectral analysis (which reveals the strength of each Fourier component) of the motion (shown in Figure 13.9b) shows a flat plateau at low frequencies with a high frequency (ω) Lorentzian decay (proportional to ω^{-2}), characteristics of thermal fluctuations in a harmonic potential. The solid line shows that the measured fluctuations are well described by theory. Similar information is obtained from the probability of finding the particle a distance x away from the beam centre, which is readily calculated from the measured trajectory, an example of which is shown in Figure 13.9c. This distribution yields directly the optical trap stiffness k since from the Boltzmann law $P(x) = A\exp(-kx^2/2k_BT)$. Finally Figure 13.9d depicts the mean-square displacement (MSD), $\langle \Delta x^2(t) \rangle = \langle |x(t) - x(0)|^2 \rangle$, of the particle as a function of time. Fitting the measured MSD gives the stiffness of the optical trap as 6 fN nm^{-1}. Consequently a typical position resolution of 1 nm equates to a force resolution of about 6 fN.

13.5.3 Dynamical complexity in colloidal gels

Particulate gels, produced by adding a non-adsorbing polymer to a stable colloidal suspension, play a wide role in industry. Gels are intrinsically complex, soft, multi-phase systems with an internal organisation or microstructure which varies with length scale. It is this structural complexity which has frustrated previous attempts to link the bulk properties of

gels to what is happening on the individual particle scale. An understanding of this local environment is critical for processing and understanding the long term stability of these materials. Particles with short-ranged attractions show an abrupt change in dynamics as the volume fraction is increased. At the arrest transition, the system transforms from a viscous liquid to a jammed, structurally disordered solid capable of sustaining a shear stress. While many commonplace materials such as foods, pesticides, coatings and cosmetics consist of colloid or protein gels, the molecular mechanism of arrest is a subject of intense scientific debate. The scientific challenge is to explain the rich variety of arrested states seen in protein and colloid gels. Optical tweezers provide a unique method to explore the very different microenvironments present within a gel.

Figure 13.10 shows the trajectory of a single spherical titania particle trapped within a gel, formed from equal sized (1.3 μm), density and index-matched poly(methyl methacrylate) spheres. The different microenvironments present within a gel sample are characterised by positioning the probe particle within a pore and at the edge of the particle chains. As is clear from the figure the different microenvironments result in very different particle dynamics. A scattering measurement, for instance, would average these different dynamics together and not reveal the true heterogeneous nature of the system.

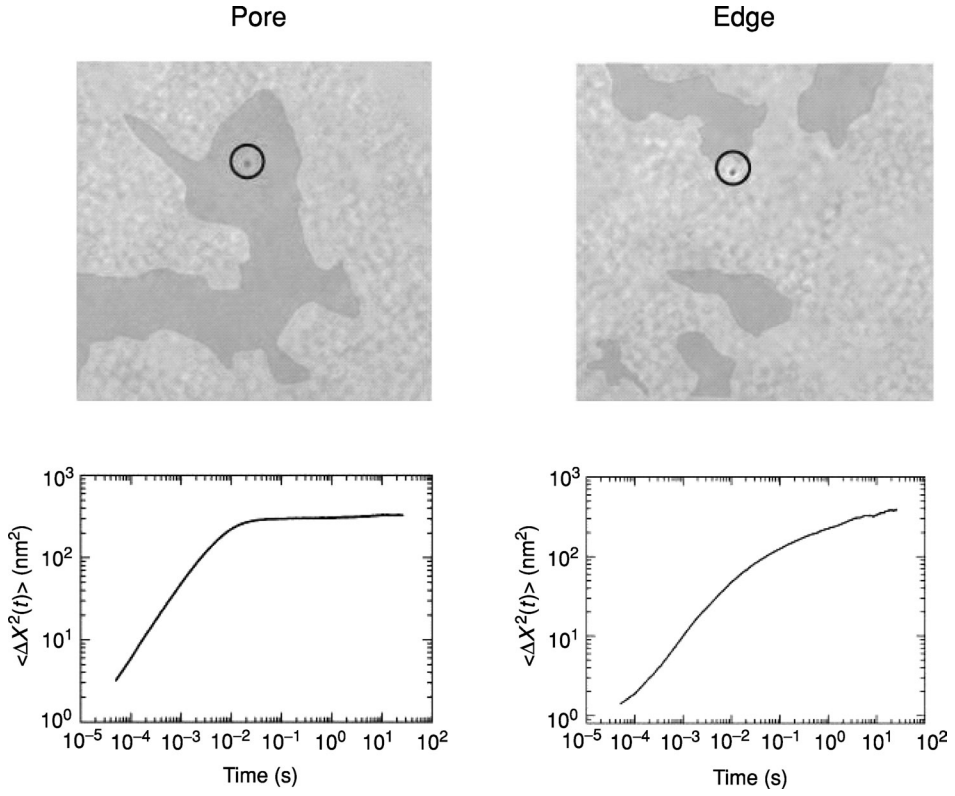

Figure 13.10 The mean-square displacement of a single colloidal particle located within the pore space and at the edge of a particle chain. Note the significant differences between the two microenvironments.

13.6 Conclusions

This chapter has provided a short introduction to the physics of optical tweezers and given a few simple applications of the technique to soft matter science. Optical tweezers can now trap and orient a large number of particles and measure their properties with high precision. The optical toolkit is now in place. In the next few years, we can expect to see these techniques rapidly developing to the point where they become mainstream, providing researchers with the ability to control the microscopic world with unparalleled precision.

References

1. Grier, D.G. (2003) A revolution in optical manipulation. *Nature*, **424** (6950), 810–816.
2. Molloy, J.E. and Padgett, M.J. (2002) Lights, action: optical tweezers. *Contemp. Phys.*, **43** (4), 241–258.
3. Dholakia, K, Spalding, G.C. and MacDonald, M.P. (2002) Optical tweezers: the next generation. *Phys. World*, **15** (10), 31–35.
4. Krauss, L.M. (1997) *The Physics of Star Trek*. Harper Collins, London.
5. van de Hulst, H.C. (1981) *Light Scattering by Small Particles*. Dover, New York.
6. Ashkin, A. (2000) History of optical trapping and manipulation of small-neutral particles, atoms, and molecules. *IEEE J. Sel. Top. Quantum Electron.*, **6** (6), 841–856.
7. Ashkin, A., Dziedzic, J.M., Bjorkholm, J.E. and Chu S. (1986) Observation of a single-beam gradient force optical trap for dielectric particles. *Opt. Lett.*, **11**, 288–290.
8. Ashkin, A. (1992) Forces of a single-beam gradient laser trap on a dielectric sphere in the ray optics regime. *Biophys. J.*, **61** (2), 569–582.
9. Harada, Y. and Asakura, T. (1996) Radiation forces on a dielectric sphere in the Rayleigh scattering regime. *Opt. Commun.*, **124**, 529–541.
10. Curtis, J.E., Koss, B.A. and Grier, D.G. (2002) Dynamic holographic optical tweezers. *Opt. Commun.*, **207** (1–6), 169–175.
11. Leach, J., Sinclair, G., Jordan, P., Courtial, J., Padgett, M.J., Cooper, J., *et al.* (2004) 3D manipulation of particles into crystal structures using holographic optical tweezers. *Opt. Express*, **12** (1), 220–226.
12. Gittes, F. and Schmidt, C.F. (1998) Interference model for back-focal-plane displacement detection in optical tweezers. *Opt. Lett.*, **23** (1), 7–9.